Startup Performance of Dry Gas Seals with Different types of Grooves Considering the Slip Flow Effects

Qiangguo Deng[1], Pengyun Song[2(✉)], Xiangping Hu[3(✉)], Hengjie Xu[2], Xuejian Sun[1],Wenyuan Mao[2]

[1] Mechanical and Electrical Engineering, Kunming University of Science and Technology, Kunming, Yunnan Province, China.

[2] Chemical Engineering, Kunming University of Science and Technology, Kunming, Yunnan Province, China.
songpengyunkm@sina.com

[3] Industrial Ecology Programme, Department of Energy and Process Engineering, Norwegian University of Science and Technology, Trondheim, Norway.
Xiangping.Hu@ntnu.no

Abstract: Finite difference method is used to solve Reynolds equation based on modified FK slip flow model. The startup performances of spiral groove, T-groove and linear groove of dry gas seal in opening stage are analyzed. The results show that in the startup stage, the slip flow effect reduces the opening force, the spiral groove is mostly affected by the slip flow effect, and linear groove is the smallest. Considering the slip flow effect, the hydrodynamic pressure effects of spiral groove is the largest, and linear groove is the smallest. This result indicates that spiral groove is easier to open with better hydrodynamic pressure effect at low speed, and linear groove is more difficult to open. Under the same conditions, the shaft speed range of spiral groove dry gas seal with obvious slip flow effect with the Knudsen number being 0.001 the smallest, followed by linear groove, and the T-groove is the largest. Our analyses and results are useful for … (need to general sentence to say that your result is useful)

Keywords: Dry gas seal, startup performance, slip flow effects, hydrodynamic pressure effect

1 Introduction

Dry gas seal is a non-contact mechanical seal, and it is widely used because of its excellent sealing performance [1]. In the startup stage, the gap (also called gas film thickness) of the seal rings increases from zero to several microns gradually. However, there are obvious slip flow effects on the seal ring faces. Therefore, it is necessary to consider the influence of slip flow effect when one analyzes the startup performance of dry gas seal.

Hydrodynamic pressure groove is arranged on the rotating ring of the dry gas seal, which can pressurize the gas film between the sealing rings and help improve the opening performance. There are many researches on the structural design and sealing performance analyses of dynamic pressure groove. Wang [2] and Li [3] respectively optimized the structural parameters of T-groove and analyzed the steady-state characteristics. Bai [4] obtained the gas film dynamic pressure and temperature distributions of T-groove end face seal under different vibration frequencies. Hu [5] and Wang [6] respectively used finite element method and simulation software to calculate the linear groove, which shows that the linear groove with proper structure can improve the opening force of the seal end face. The team of Song [7-9] analyzed the sealing performance of spiral groove, T-groove and linear groove in steady state by finite difference method (FDM) or analytical method. Ruan [10], Yin [11] and Zhao [12] used FEM to solve the modified Reynolds equation considering the slip flow effect, and they verified that the spiral groove dry gas seal has obvious slip flow effect under low pressure and low speed.

At present, most researchers mainly focuses on the optimization of groove structures, the analysis of steady-state characteristics and the performance analysis considering the slip flow effects in the stable operation stage, and there are few literatures on the influence of the slip flow effects on the sealing opening force, leakage rate and opening speed during the startup stage. In this paper, the opening force, leakage rate and opening speed of spiral groove, T groove and linear groove in the startup stage considering the influence of slip flow effects are analyzed by a numerical analysis method. The research provides reference for the reasonable evaluation of the influence of slip flow effects on the performance of dry gas seals in the startup stage.

2 Slip flow models

In 1909, Knudsen[13] defined the fluid flow area according to the degree of gas deviation from the continuum flow, and proposed a characteristic parameter that characterizes the slip flow effects—Knudsen number(*Kn*). Knudsen number represents the degree of rarefaction of the gas, the larger the value, the more obvious the rarefaction effect.

Knudsen number is defined as:

$$K\mathrm{n} = \frac{\lambda}{h} \tag{1}$$

where h is gas film thickness between rotating ring and stationary ring, λ is molecular mean free path and it is defined as:

$$\lambda = \frac{\mu\sqrt{2\pi R_c T_0}}{2p} \tag{2}$$

Where R_c is gas constant, M is molecular mass, p is pressure, T_0 is characteristic temperature, μ is viscosity.

According to Eq.(1) and Eq.(2), at low speed, small film thickness, and low pressure, the slip flow effect is more obvious. Therefore, it is necessary to consider the slip flow effects when solved the pressure distribution of gas film governing equation in the startup stage.

2.1 FK-slip flow model

Fukui and Kaneko [14] proposed a modified Reynolds equation to study the slip flow effect by introducing flow factors derived from linearized Boltzmann equation. For an isothermal, compressible lubricant, ideal gas behavior，the modified Reynolds equation is given by:

$$\frac{1}{r}\frac{\partial}{\partial r}\left(Q\frac{rph^3}{12\mu}\frac{\partial p}{\partial r}\right)+\frac{1}{r}\frac{\partial}{\partial\theta}\left(Q\frac{ph^3}{12\mu r}\frac{\partial p}{\partial\theta}\right)=\frac{\omega}{2}\frac{\partial(ph)}{\partial\theta}+\frac{\partial(ph)}{\partial t} \tag{3}$$

where r is radius, t is time, h is gas film thickness, ω is angular velocity.

The steady-state condition:

$$\frac{1}{r}\frac{\partial}{\partial r}\left(Qrh^3\frac{\partial p^2}{\partial r}\right)+\frac{1}{r^2}\frac{\partial}{\partial\theta}\left(Qh^3\frac{\partial p^2}{\partial\theta}\right)=12\mu\omega\frac{\partial(ph)}{\partial\theta} \tag{4}$$

where Q, the relative flow rate coefficient is defined as:

$$Q = Q_p / Q_c \tag{5}$$

where Q_p is flow rate of the Poiseuille flow, and Q_c is flow rate of the continuum Poiseuille flow, the calculation results are shown as follows:

$$\begin{cases} Q_c = D/6 \\ \begin{cases} Q_p = D/6 + 1.0162 + 1.0653/D - 2.1354/D^2 \left(D > 5\right) \\ Q_p = 0.13852D + 1.25087 + 0.15653/D - 0.00969/D^2 \left(0.15 < D < 5\right) \\ Q_p = -2.22919D + 2.10673 + 0.01653/D - 0.0000694/D^2 \left(0.01 < D < 0.15\right) \end{cases} \end{cases} \tag{6}$$

where *K*n is Knudsen number, *D* is inverse Knudsen number, which can be defined as:[15]

$$D = \frac{\sqrt{\pi}}{2Kn} \tag{7}$$

$$D = D_0 ph \tag{8}$$

where D_0 is characteristic inverse Knudsen number defined as:

$$D_0 = \frac{p_a h_0}{\mu\sqrt{2R_c T_0}} \tag{9}$$

Where p_a is atmospheric pressure.

2.2 The 1st order and 2nd order slip flow models

The flow rate of the Poiseuille folw, Q_{p1} and Q_{p2} for the 1st order and 2nd order slip flow models[16]:

$$\begin{cases} Q_{p1} = D/6 + \dfrac{a\sqrt{\pi}}{2} \\ Q_{p2} = D/6 + \dfrac{a\sqrt{\pi}}{2} + \dfrac{a\pi}{4D} \end{cases} \tag{10}$$

$$a = \frac{2-\varepsilon}{\varepsilon} \tag{11}$$

where ε is the accommodation coefficient representing the portion of the molecules inside the Knudsen layer that collide with the wall，which usually is taken to be 1. *a* is the surface correction coefficient. The model coefficients χ and *v* of modified Reynolds equation are listed in table 1.

Table 1 The model coefficients χ and *v* of modified Reynolds equation

Models	χ	*v*	Models	χ	*v*
1st order slip flow model	6*a*	0	New 1st order slip flow model	4*a*	0
2nd order slip flow model	6*a*	6*a*	New 2nd order slip flow model	4*a*	3

2.3 Wu lin's slip flow model

After using the assumptions that the gas is ideal and the gas layer is isothermal, Wu lin[17] obtain a slip lubrication equation:

$$\frac{\partial}{\partial X}\left[\left(PH^3 + \chi K_n H^2 + \nu K_n^2 \frac{H}{P}\right)\frac{\partial P}{\partial X}\right] + \frac{\partial}{\partial Y}\left[\left(PH^3 + \chi K_n H^2 + \nu K_n^2 \frac{H}{P}\right)\frac{\partial P}{\partial Y}\right] = \Lambda_x \frac{\partial}{\partial X}(PH) + \Lambda_y \frac{\partial}{\partial Y}(PH) \tag{12}$$

where *P* is non-dimension pressure, *H* is non-dimension gas thickness, Λ is bearing number.

The new 1st order and 2nd order slip flow models are derived from the characteristics of two-dimensional molecular dynamics:

$$\begin{cases} Q_{p1} = D/6 + \left(\frac{2}{3}\right)\frac{a\sqrt{\pi}}{2} \\ Q_{p2} = D/6 + \left(\frac{2}{3}\right)\frac{a\sqrt{\pi}}{2} + \left(\frac{1}{2}\right)\frac{a\pi}{4D} \end{cases} \tag{13}$$

2.4 Huang's slip flow model

Huang Ping[16] obtained the fitting formula according to the numerical results of the FK model and the linearized Boltzmann equation in the wide watershed are follows:

$$Q_p = D/6 + 1.0162 + 0.40134\ln\left(1 + 1.2477/D\right) \tag{14}$$

2.5 1+6*K*n-slip flow model

Burgdorfer[18] proposed the modified Reynolds equation consider the slip flow effects as follows:

$$\frac{\partial}{\partial\theta}\left(ph^3\frac{\partial p}{\partial\theta}\left(1+6K_n\right)\right) + r\frac{\partial}{\partial r}\left(ph^3\frac{\partial p}{\partial r}\left(1+6K_n\right)\right) = 6\eta\omega r\frac{\partial\left(ph\right)}{\partial\theta} \tag{15}$$

To write Eq.(15) in non-dimensional as follows:

$$\frac{1}{R^2}\frac{\partial}{\partial\theta}\left(\frac{\partial P}{\partial\theta}\left(PH^3 + 6K_nH^2\right)\right) + \frac{1}{R}\frac{\partial}{\partial R}\left(\frac{\partial P}{\partial R}\left(RPH^3 + 6K_nRH^2\right)\right) = \Lambda\frac{\partial\left(PH\right)}{\partial\theta} \tag{16}$$

3 Calculation of sealing performance parameters

The boundary conditions are the prescribed inner and outer pressure given by:

$$\begin{cases} r = r_i, p = p_i \\ r = r_o, p = p_o \end{cases} \tag{17}$$

The cyclic boundary conditions can be described by the following:

$$p\left(r,\theta\right) = p(r,\theta + 2\pi/N_g) \tag{18}$$

The total opening force can be calculated by integrating the pressure over the seal face area as:

$$F_{\mathrm{o}} = \int_0^{2\pi}\int_{r_{\mathrm{i}}}^{r_{\mathrm{o}}} p(r)r\mathrm{d}r\mathrm{d}\theta \tag{19}$$

The closing force of dry gas seal:

$$F_{\mathrm{close}} = p_{\mathrm{i}}\pi(r_{\mathrm{b}}^2 - r_{\mathrm{i}}^2) + p_{\mathrm{o}}\pi(r_{\mathrm{o}}^2 - r_{\mathrm{b}}^2) + p_{\mathrm{sp}}\pi(r_{\mathrm{o}}^2 - r_{\mathrm{i}}^2) \tag{20}$$

where r_{i}, r_{o}, r_{b} is inner and outer radius and balance radius, p_{sp} is spring pressure.

The leakage rate can be obtained in the following way:

$$Q_L = \int \frac{Mp(r)rh^3}{12\mu R_r T} \frac{\partial p}{\partial r} \mathrm{d}\theta \tag{21}$$

4 Selection model and verification

The finite difference method is used to discretize the governing equation of gas film pressure in Eq.(4), which is numerically calculated by MATLAB software. Firstly, the geometric parameters, operation parameters, boundary conditions and initial calculation parameters of the calculation model are set. The pressure distribution equation is solved by over-relaxation iteration method. Then convergence is judged when solving, if the convergence condition is met, the iteration is stopped; otherwise, the current pressure value at each point is taken as the initial condition, and the iteration is continued until the convergence condition is met.

4.1 Selection slip flow model

The lubrication characteristics of micro-scale fluid considering slip flow effects are analyzed, and the slip flow models mentioned above are compared with the experimental data of Jiang[19], hoping to find a slip flow model more in line with the actual working conditions. Taking the bionic bundle groove in reference [19] as the research object, the opening force law of each slip flow model in the film thickness range of 0.4~5.5 μm are calculated with the experimental model and working condition parameters.

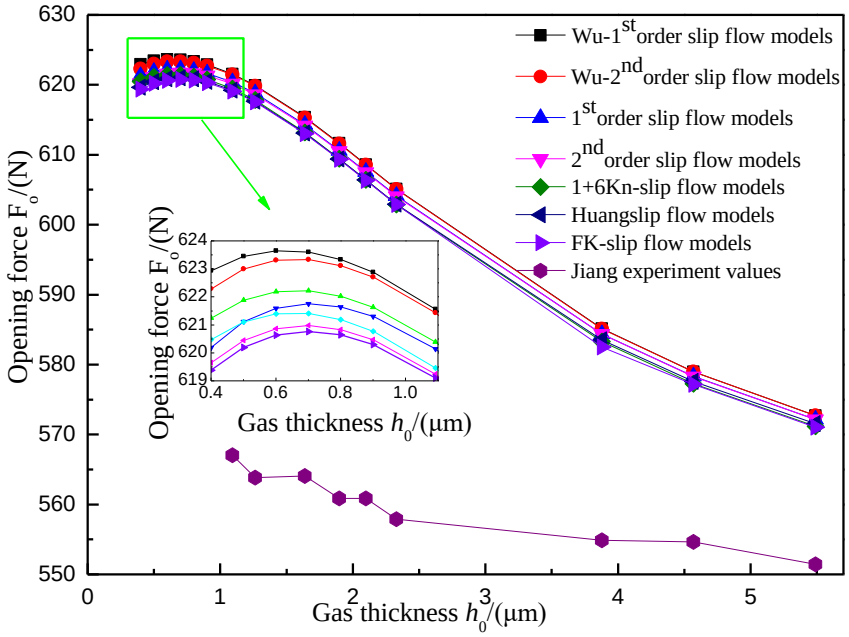

Fig.1 Opening force of various slip flow models

By analyzing Figure 1, the maximum deviation between the opening force of various slip flow models and the experimental data in literature is 8.3%. The numerical calculation of the slip flow model is isothermal and steady-state model, and the gas film temperature, seal ring deformation and various unstable factors in actual operation, such as rotating ring channeling and machining error, are not considered, so there is a certain deviation between the numerical calculation and the experimental data. The maximum deviation of opening force between various

slip flow models is 0.47%, and the data of FK slip flow model is the closest to the literature data, so FK slip flow model is selected to characterize the slip flow effects of dry gas seal.

4.2 Verification of dry gas seal opening characteristic model

In order to verify the correctness of the program calculation, the calculation results of Ruan [20] are selected as the reference object, and the literature data comes from the finite element method to solve Reynolds equation modified based on FK slip flow model. The comparative data are shown in Figure 2.

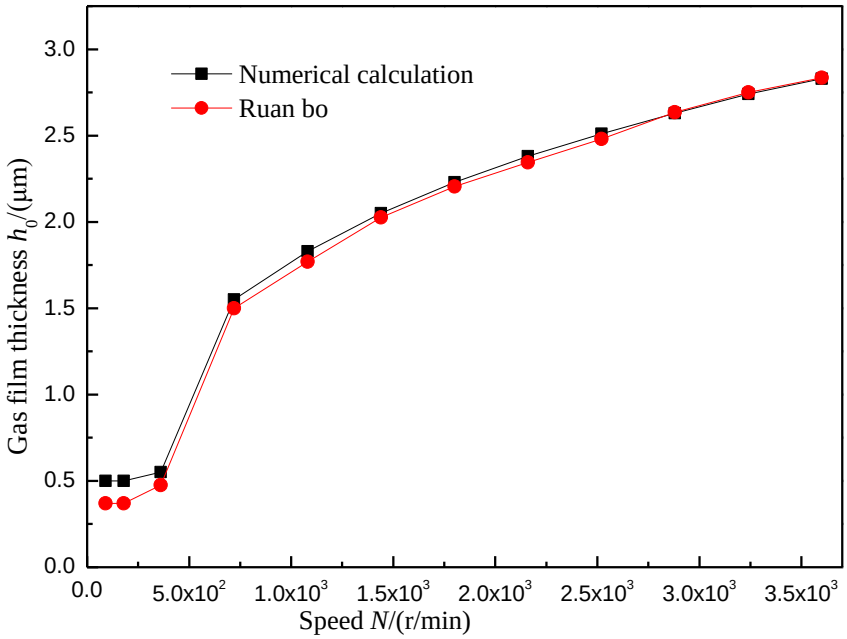

Fig.2 Verification of calculation program

It can be seen from Figure 2 that, except for the difference at low shaft speed, when the shaft speed is higher than 1080 r/min, the numerical results are very close to the literature values. The difference is may be caused by the different evaluation criteria of opening film thickness. Reference [20] defines the opening film thickness as 3.7 times of the comprehensive deviation of the surface roughness of the seal faces, where Gaussian distribution probability of asperity height distribution on rough surfaces is 99.97%, that is, $h_0=3.7\sigma_s=3.7\times0.1=0.37$ μm, where σ_s is comprehensive deviation of surface roughness

In this paper, the opening film thickness is determined according to the contact force. According to the GW contact model, the relationship between the film thickness of the model in literature [20] and the contact force of the seal end faces can be calculated. It can be seen that when the opening film thickness h_0=0.37 μm, the contact force 206 N，being much more than zero N. When the opening film thickness h_0=0.52 μm, the contact force 0.28 N, and the proportion of the asperity contact force in the opening force (contact force/opening force) is 0.03%, that is, the non-contact part of the opening force accounts for 99.97%. At this time, it can be seen that the contact force is almost zero, which means that the sealing end face has no contact and has been completely non-contact. Therefore, when the contact force is zero, the film thickness is defined as the opening film thickness. That probably is the main reason for the deviation between them in Figure 2 at the low speed period. With the increasing of shaft speed, when the seal end faces are completely non-contact, the deviation between them gradually decreases, and when the speed

being 3600 r/min, the deviation between them is only 0.18%. Therefore, the calculation program in this paper is reasonable.

5 Results and Discussion

5.1 Examples

Spiral groove, T-groove and linear groove are selected to analyze the opening characteristics of dry gas seal. The groove structure and sealing parameters of three types of grooves have been given respectively in Figure 3 and Table 2. In order to intuitively compare the opening performance of different groove structures, the inner and outer diameters of three types of grooves are the same，and the groove-to-table ratio of each grooves is 1. That is, the circumferential length and area of the groove and the table are respectively equal. For T- groove, it means that the sum of the circumferential length of the large groove and the small groove is equal to the sum of the circumferential length of the large table and the small table.

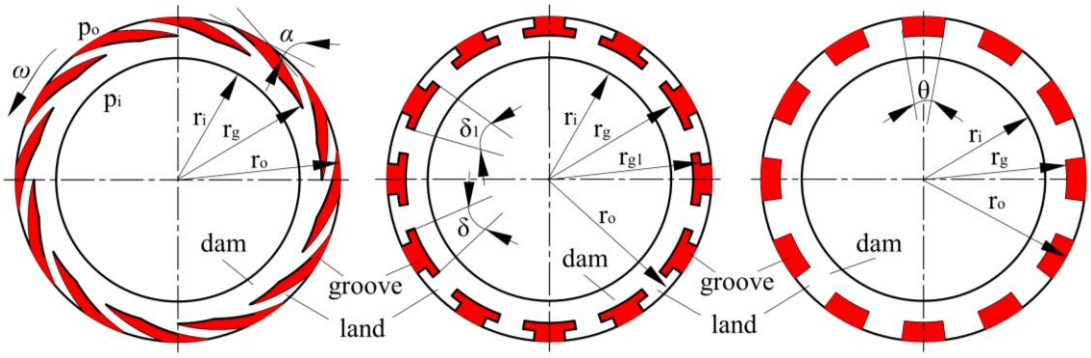

(a) Spiral groove (b) T-groove (c) Line groove

Fig.3 Dry gas seal groove structure

Table 2 Dry gas seal parameters

Parameters	Values	Parameters	Values
Outer radius, r_o/mm	77.78	Spiral groove angle, α/°	15
Inner radius, r_i/mm	58.42	Number groove, N_g/μm	12
Groove inner radius, r_g/mm	69	Groove depth, h_g/μm	5
Balance radius, r_b/mm	61.3	Ambient pressure, p_i/MPa	0.101
Groove middle radius, r_{g1}/mm	73.39	Sealed gas pressure, p_o/MPa	4.5852
Groove-to-land ratio , γ	1	Gas constant, R_r/J/ (mol·K)	8.3144
L-groove central angle, θ/°	15	Viscosity, $\mu/10^{-6}$pa·s	18.6
T-groove large central angle, δ/°	20	Molecular mass,M/g/mol	29
T-groove small central angle, δ_1/°	10.3	Temperature, T/K	303.15

5.2 Relative Errors

Based on the modified Reynolds equation of FK slip flow model, the sealing parameters such as opening force, leakage rate and opening shaft speed of seal end face are calculated. In order to directly reflect the influence degree of the slip flow effects on the opening performance, the

relative errors of the opening parameters of each type groove with or without slip flow effect are defined:

E_1= [(Opening speed of slip flow - Opening speed of non-slip flow)/Opening speed of non-slip flow] × 100%

E_2= [(Equilibrium film thickness of non-slip flow - Equilibrium film thickness of slip flow)/Equilibrium film thickness of non-slip flow] × 100%

E_3= [(Equilibrium speed of slip flow - Equilibrium speed of non-slip flow)/ Equilibrium speed of non-slip flow] × 100%

E_4= [(Leakage rate of non-slip flow - Leakage rate of slip flow)/Leakage rate of non-slip flow] × 100%

5.3 Startup Performance Analysis

In the startup stage of dry gas seal, the end faces of seal rings go through the process of contact to non-contact to stable working film thickness, and the gas film thickness is dynamically increasing. This section is based on the operating condition parameters in Table 2, and the opening film thickness is taken as 0.52 μm. At this time, the contact force relative to the opening force accounts for 0.03%. Table 3 shows the startup performance parameters of the three types of grooves. The opening speed can be seen that the spiral groove being 950 r/min, T-groove being 4340 r/min, and the linear groove being 5030 r/min when the slip flow effects is considered. Compared with T-groove and linear groove, the opening speed of spiral groove dry gas seal is the lowest. It shows that the spiral groove dry gas seal is easiest to open and the linear groove needs highest shaft speed to open, which proves that the spiral groove has the best hydrodynamic pressure effect and the linear groove has the worst.

When considering the effect of slip flow, the opening speed and leakage rate of the same type groove are larger than those of the non-slip flow calculation model. Because the film thickness is small in the startup stage, and the slip flow effect is obvious, or the effective viscosity of the gas film is reduced [7], and the viscous shear force is weakened, which leads to the reduction of the hydrodynamic pressure effect of the gas film and the opening force. A higher opening speed is required to reach the opening film thickness. The opening speed related errors of the three types groove due to slip flow effects are as follows: Spiral groove E_1=17.89%, T-groove E_1=17.05% and linear groove E_1=17.34%, which means that the influence of slip flow effect on spiral groove is higher than those of T-groove and linear groove in the opening stage.

Table 3 Startup performance when gas film thickness h_0=0.52 μm

	Spiral groove		T-groove		Linear groove	
Parameters	Non- slip flow	Slip flow	Non- slip flow	Slip flow	Non- slip flow	Slip flow
Speed N/(r/min)	780	950	3600	4340	4158	5030
Leakage rate Q_L /(10^{-6}kg/s)	3.32	3.81	3.27	3.7	3.27	3.71

According to the quasi-steady state concept, when the opening force is equal to the closing force, the seal ring is in equilibrium state in the non-contact period, the shaft speed at this time is called the equilibrium speed, and the seal end face gap is the equilibrium film thickness at this time. The opening gas film (h_0=0.52 μm) is the first one of the equilibrium film thicknesses.

Figure 4 shows the startup performance parameters of the three types of grooves with increasing shaft speed. It can be seen that for the same type groove and the same speed, the slip flow effects reduces the equilibrium film thickness and resulting in less leakage rate. For example,

for the spiral groove dry gas seal with shaft speed of 6000 r/min, without considering the slip flow effect, the equilibrium film thickness h_0=1.9 μm, the leakage rate Q_L =2.82×10^{-4} kg/s. And the slip flow effect is considered, the equilibrium film thickness h_0=1.86 μm, the leakage rate Q_L=2.73×10^{-4} kg/s. The equilibrium film thickness related errors is E_2=2.1%, and the leakage rate related errors is E_4=3.2%. In order to maintain the equilibrium state where the opening force is equal to the closing force, the equilibrium film thickness considering the slip flow effect will automatically decrease to supplement the opening force loss caused by the slip flow effect. At the same time, the equilibrium film thickness considering the slip flow effects is smaller than the equilibrium film thickness without the slip flow effect, and the leakage rate corresponding to the small film thickness is naturally smaller than that of the large film thickness.

When the shaft speed 950(r/min), the equilibrium film thickness of spiral groove of day gas seal h_0=0.67 μm without slip flow effect and h_0=0.52 μm with slip flow effect, and the equilibrium film thickness related errors being E_2=22.39%. Comparing the equilibrium film thickness related errors caused by slip flow effect at shaft speed 950 r/min (E_2=22.39%) and 6000 r/min (E_2=2.1%). It found that with the increasing of the shaft speed, the film thickness gradually increases, and the slip flow effect becomes smaller and smaller, so the influence of slip flow effect on startup performance of dry gas seal becomes lower and lower.

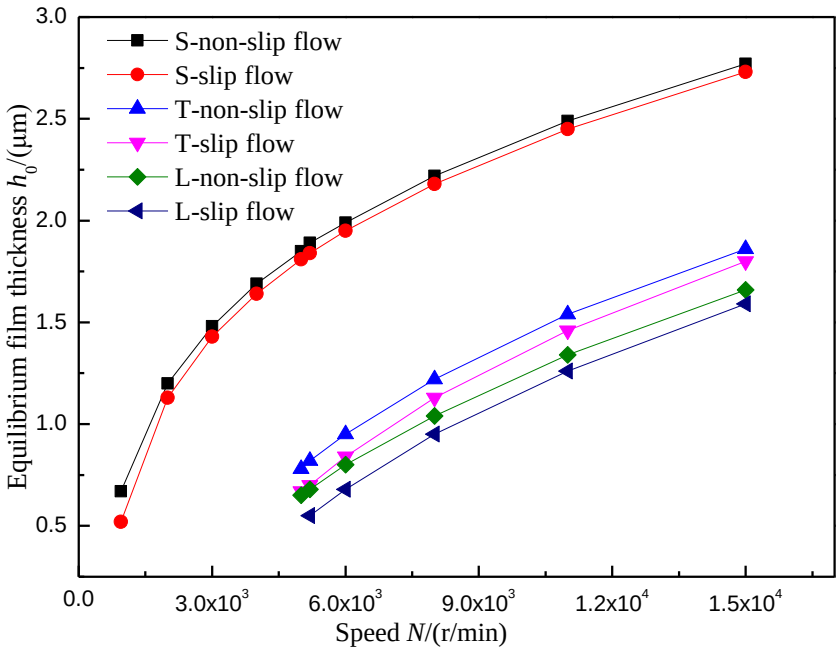

(a) h_0 *vs* N

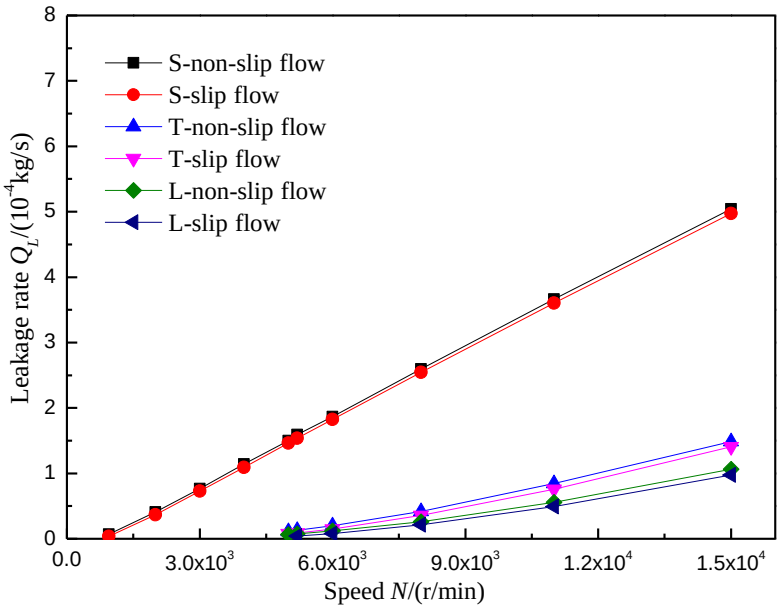

(b) Q_L *vs* N

Fig.4 Startup parameters of different grooves on quasi-steady state

Table 4 shows the working parameters of three types groove when the equilibrium film thickness h_0=2 μm. The equilibrium speed of spiral groove is much lower than that of T-groove and linear groove, which is determined by the difference of hydrodynamic pressure effect of groove structure. It shows that spiral groove has much higher hydrodynamic pressure effect than T-groove and linear groove, and has better sealing performance. However, the leakage rate of spiral groove is slightly higher than the other two types of grooves, which is also related to the groove structure. The pressure at the root of spiral groove is concentrated, resulting in greater pressure, which makes the leakage rate larger, while the pressure distribution of T-groove and linear groove is relatively scattered, and the leakage rates of the two grooves are closer.

When the equilibrium film thickness h_0=2 μm, the equilibrium speed related errors of each type groove due to slip flow effects is analyzed. The results show that the spiral groove E_3=4.9%, the T-groove E_3=4.2% and the linear groove E_3=4.2%, which means that the influence of slip flow effect on the spiral groove is still higher than that on the T-groove and the linear groove.

Table 4 Working performance when equilibrium film thickness h_0=2 μm

	Spiral groove		T-groove		Linear groove	
Parameters	Non-slip flow	Slip flow	Non-slip flow	Slip flow	Non-slip flow	Slip flow
Speed N/(r/min)	6050	6400	17000	17800	20300	21300
Leakage rate Q_L (10^{-4}kg/s)	1.89	1.97	1.85	1.92	1.85	1.92

Figure 5 shows the variation law of gas film opening force and leakage rate with shaft speed when the opening film thickness h_0=0.52 μm. It can be seen that for the same type groove and the same speed, the slip flow effects decreases the gas film opening force and increases leakage rate. When the opening force of the sealing ring is greater than the closing force, the sealing end faces can be completely disconnected and the sealing ring can be opened. Under the same shaft speed, the opening force and leakage rate of spiral groove are larger than those of T-groove and linear groove. Spiral groove can open the sealing ring faster, followed by T-groove, while the linear groove is the slowest, which needs a larger speed to improve the opening force.

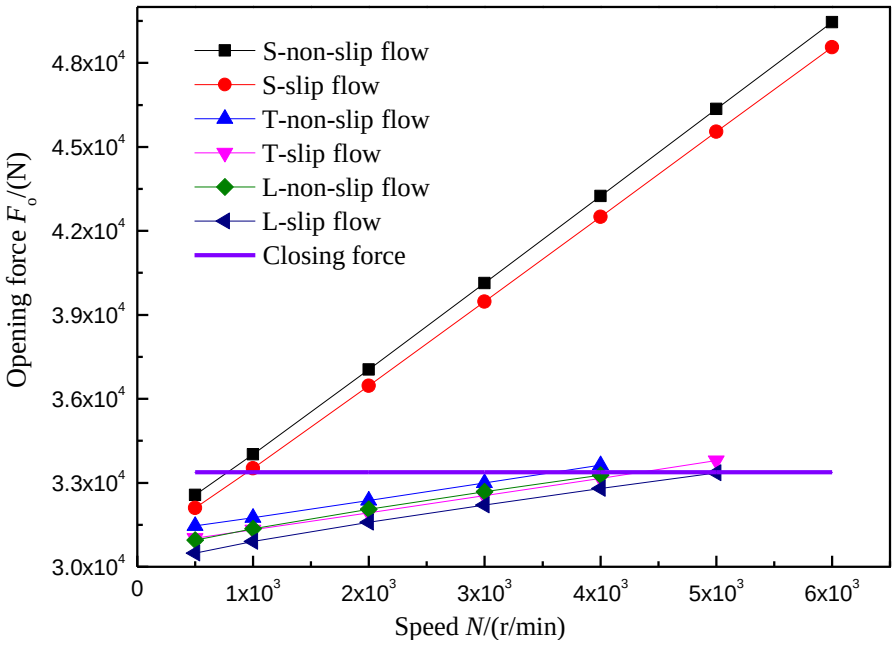

(a) F_o *vs* N

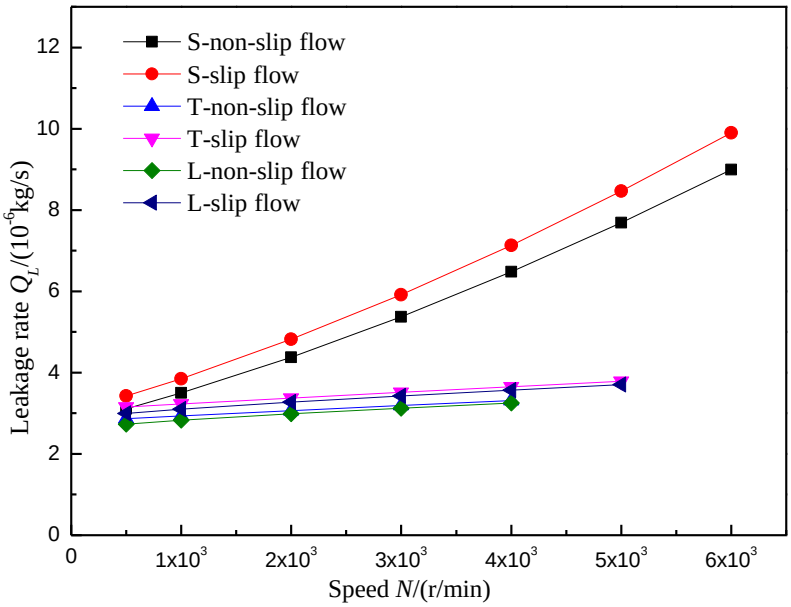

(b) Q_L *vs* N

Fig.5 Performance performance of different grooves (h_0=0.52 μm)

5.4 Judgment of influence interval of slip flow

The startup performance of the dry gas seal are obviously affected by the slip flow effects, but with the increasing of the shaft speed, the film thickness gradually increases, and the influence of the slip flow effects on the opening performance of the seal gradually decreases. Therefore, the sealing performance of the dry gas seal in the startup stage is discussed. It is necessary to define the scope of the slip flow phenomenon, that is, to clarify the relationship between the sealing parameter and the characteristic parameter of slip flow-Knudsen number, and to clarify whether slip flow effect should be considered in calculation in the opening stage.

From the definition of the Knudsen number, it is known that the pressure and temperature distribution, viscosity and gas film thickness of the sealing end faces directly determine the

influence range of the slip flow effect. Knudsen defined the obvious slip flow effect in the range of 0.001≤Kn≤0.1. In this paper, the working condition parameters of dry gas seal are from the Gabriel literature [21] .The influence interval of slip flow effect in different dynamic pressure grooves is analyzed. For the facilitate of calculation, the average Knudsen number of a certain instantaneous equilibrium film thickness is taken as the analysis object, and this value is the average value of the Knudsen number of each calculation node in the finite difference method.

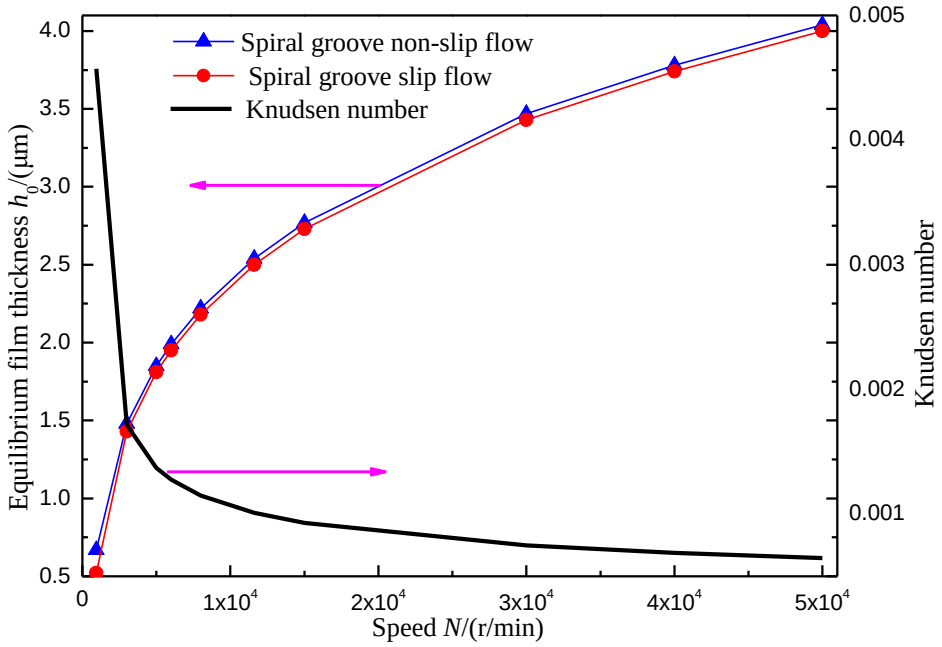

(a) Spiral groove

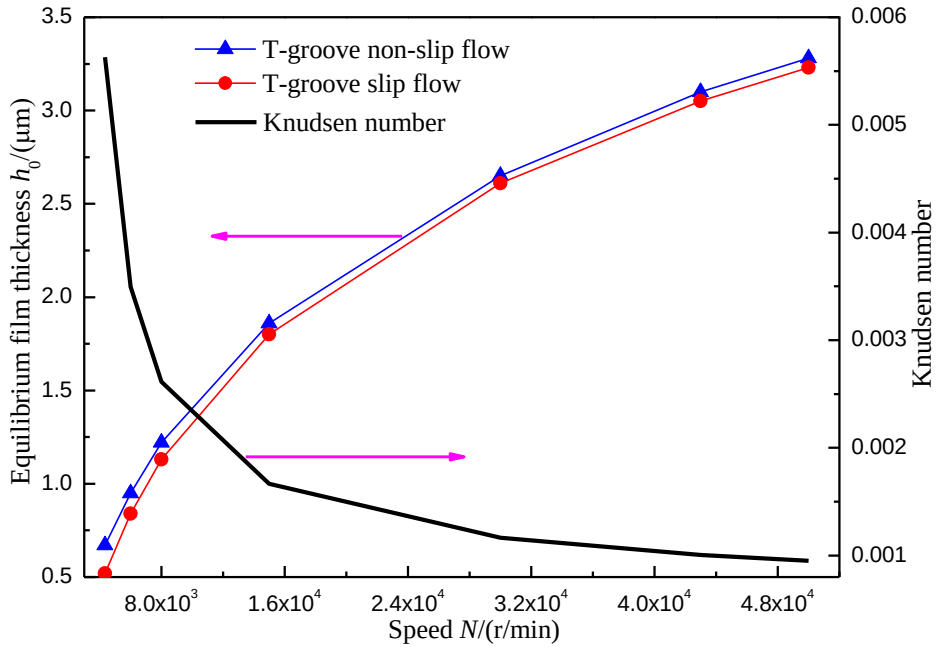

(b) T-groove

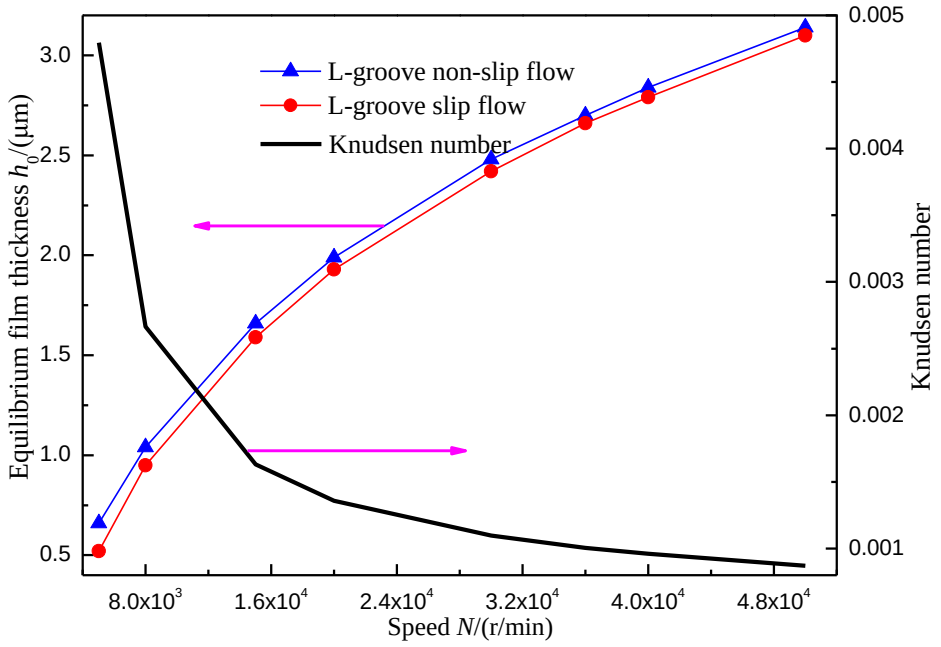

(c) Linear groove

Fig.6 The equilibrium film thickness and Knudsen number of different grooves

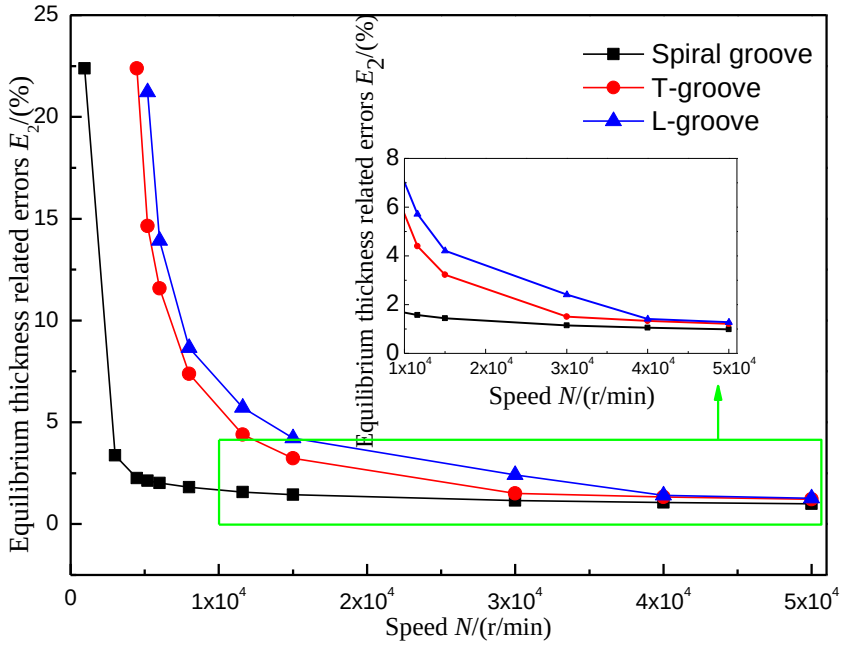

Fig.7 The equilibrium film thickness related errors of different grooves

Figure 6 show the variation of the equilibrium film thickness and Knudsen number of the spiral groove, T-shaped groove and linear groove with the shaft speed. It can be seen that as the shaft speed increases, the equilibrium film thickness of the three types groove gradually increases, while the average Knudsen number gradually decreases, and the Knudsen number of the three types grooves dry gas seals decreases rapidly with the increasing in shaft speed. The equilibrium film thickness related errors of the three types groove with influence of the slip flow effects are shown in Figure 7, which reduces with the increasing of the shaft speed.

Table 5 The equilibrium film thickness related errors of three types of grooves

	Spiral groove	T-groove	Linear groove

Parameters	Opening speed	Equilibrium speed	Opening speed	Equilibrium speed	Opening speed	Equilibrium speed
speed N/(r/min)	950	12150	4340	43800	5030	37250
Knudsen number	0.0049	0.001	0.0059	0.001	0.0051	0.001
E_2/(%)	22.39	1.55	22.39	1.29	22.21	1.82

Table 5 shows the Knudsen number and the equilibrium film thickness related errors E_2 of the three types of grooves dry gas seals at the opening speed and an equilibrium speed with Kn=0.001 for each type groove. It can be seen that these two parameters are relatively large in the opening speeds, indicating that the influence of slip flow effects are more obvious. However, the influence of the slip flow effects gradually reduces with the increasing of the shaft speed resulting in the equilibrium film thickness related errors E_2 gradually decreasing. when Kn $\leq$ 0.001, the equilibrium film thickness related errors E_2 of the three types of grooves are all very small. That means that Kn=0.001 being an indicator for considering the slip-flow effect is reasonable. Knudsen defined that the slip flow effects being very small at this situation, which can be ignored. According to the definition of Knudsen, the maximum speed with the slip flow effect under the same working conditions: spiral groove being 12150 r/min, T-groove being 43800 r/min, Linear groove being 37250 r/min. It can be seen that the spiral groove dry gas seal is most affected compared to the T-groove and linear groove dry gas seals at low speeds. The equilibrium film thickness related errors decreases rapidly with the increase of the shaft speed, and the descending speed is greater than that of the linear groove and the T-groove. This indicates that under the same conditions, the spiral groove dry gas seal is significantly affected by the slip flow effect in the startup stage, and the shaft speed range is the narrowest, followed by the linear groove, and the T-groove is the widest.

6 Conclusions

(1) Comparing with the experimental data in the literature, the FK model is more suitable to the slip flow effect in the dry gas seal.

(2) In the startup stage of dry gas seal, the slip flow effect reduces the opening force of the same groove. Spiral groove is most affected by slip flow effect, followed by T-groove and linear groove is the least.

(3) Considering the slip flow effects, the hydrodynamic pressure effect from large to small is spiral groove to T-groove to linear groove, which is determined by the groove structure.

(4) The variation law of the influence of the slip flow effect on the equilibrium film thickness of the dry gas seal with the increasing of the shaft speed is given. For the same type groove and the same speed, the slip flow effect reduces the equilibrium film thickness and resulting in less leakage rate. With the increasing of the shaft speed, the slip flow effect becomes smaller and smaller. The spiral groove dry gas seal is significantly affected by the slip flow effect, and the slip flow speed range is the narrowest, followed by the linear groove, and the T-groove widest.

7 Acknowledgement

The research is supported by National Natural Foundation of China (granted no. 51465026) and Program of Yunnan Provincial Natural Science Fund Project (granted no. 202101AU070019)

References

1. Gu Yong Quan. Practical technology of mechanical seal[M]. Machinery Industry Press, 2001. (in Chinese)
2. Wang Yan, Sun Jianjun, Tao Kai, et al. Numerical Analysis of T-Groove Dry Gas Seal and Groove Optimization [J]. Tribology, 2014, 34(4):420-427. (in Chinese)
3. Li, Tao Zi, Zhang Qiu Xiagn, Cai Ji Ning, et al. Steady-state performance analysis of t-shape groove dry gas seals by a finite element method [J]. Journal of Beijing University of Chemical Technology, 2003, 30(2):58-62. (in Chinese)
4. Bai Shao Xian, Wei Jia, Zu De Lei, et al. Thermoelastohydrodynamic Gas Lubrication of T-Groove Face Seals: Stability of Sealing Film[J]. Tribology, 2019, 39(2):131-139. (in Chinese)
5. Hu Dan Mei, Wu Zong Xiang. Analysis and Calculation of the Gas Seal on the End Face of the Linear Groove[J]. Fluid Machinery, 1996, 24(9):16-22. (in Chinese)
6. Wang He Sun, Chen Ci Chang, Huang Ze Pei, et al. Numerical Simulation of the Face Flow Field on Radial Groove Dry Gas Seal[J]. Chinese Hydraulics and Pneumatics, 2004, 10:21-23. (in Chinese)
7. Song Peng Yun, Zhang Shuai. An approximately analytical method of characteristics of spiral groove dry gas seals under slip flow conditions[J]. Journal of Drainage and Irrigation Machinery Engineering, 2014, 32(10):877-882. (in Chinese)
8. Zhang Xuan, Song Peng Yun. Theoretical analysis of the operating characteristics of T-groove dry gas seal at the slow speed conditions[J]. Lubrication Engineering, 2010, 35(10):49-54. (in Chinese)
9. Song Peng Yun, Cheng Kang Min. Numerical analysis of the pressure on the face of a radial groove mechanical deal for gas[J]. Journal of Yunnan polytechnic university, 1999, 15(3):1-6. (in Chinese)
10. Ruan Bo. Finite element analysis of the spiral groove gas face seal at the slow speed and the low Pressure conditions-slip flow consideration[J]. Tribology Transactions, 2000, 43(3): 411-418.
11. Yin Xiao Ni, Peng Xu Dong. Finite element analysis of a dry gas seal under slip flow conditions[J]. Lubrication Engineering, 2006(04):60-61+64. (in Chinese)
12. Zhao Yue, Song Peng Yun, Li Wei, et al. The operation characteristics of spiral groove gas face seal at the slow speed—theory analysis[J]. Lubrication Engineering, 2005,171(5):70-73. (in Chinese)
13. Knudsen M. Die Gesetze der MolekularstrÖmung und der inneren ReibungsstrÖmung der Gase durch RÖhrenn[J]. Annalen der Physic, 1909, 333(1): 75-130.
14. Fukui S, Kaneko R . A Database for Interpolation of Poiseuille Flow Rates for High Knudsen Number Lubrication Problems[J]. Asme J Tribology, 1990, 112(1):78-83.
15. Wen Shi Zhu, Huang Ping. Principles of Tribology [M]. 3rd edition. Beijing: Tsinghua University Press, 2008: 22-29. (in Chinese)
16. Huang Ping. Lubrication numerical calculation method [M]. Beijing: Higher Education Press, 2012: 93-97. (in Chinese)
17. Wu Lin. Physical modeling and numerical simulations of the slider air bearing problem of hard disk drives[D].Berkley: University of California, 2001.
18. Burgdorfer A.The Influence of the Molecular Mean Free Path on the Performance of Hydrodynamic Gas Lubricated Bearings[J].journal of Basic Engineering. 1959, 81:94-98.
19. Jiang Jin Bo. theoretical and experiental study of the bionic design of grooved surface of a high speed dry gas seal[D]. Hangzhou, Zhejiang University of Technology, 2016. (in Chinese)
20. Ruan B. Numerical Modeling of Dynamic Sealing Behaviors of Spiral Groove Gas Face Seals[J]. Journal of Tribology, 2002, 124(1):186-195.

21. Gabriel R P. Fundamentals of spiral groove noncontacting face seals[J]. Lubrication Engineering, 1994, 50(3):215-224.